

Title	Studies on the thermal problems of memory cores at their high-speed performances
Sub Title	
Author	北川, 節(Kitagawa, Misao) 横山, 光男(Yokoyama, Teruo) 海老原, 規郎(Ebihara, Norio)
Publisher	慶応義塾大学藤原記念工学部
Publication year	1967
Jtitle	Proceedings of the Fujihara Memorial Faculty of Engineering Keio University (慶応義塾大学藤原記念工学部研究報告). Vol.20, No.78 (1967.) ,p.62(6)- 78(22)
JaLC DOI	
Abstract	This paper describes a measuring method of the surface temperature of small bodies somewhat above the room temperature and the temperature dependence of switching characteristics of memory cores. The temperature rise of memory cores at high-speed performances has been observed by the method using phosphors, and the relations between the surface temperature rise and the effective temperature rise of cores are obtained. Besides, thermally available criterions are also proposed to estimate the factors affecting the limitations of the cycle time of storage.
Notes	
Genre	Departmental Bulletin Paper
URL	https://koara.lib.keio.ac.jp/xoonips/modules/xoonips/detail.php?koara_id=KO50001004-00200078-0006

慶應義塾大学学術情報リポジトリ(KOARA)に掲載されているコンテンツの著作権は、それぞれの著作者、学会または出版社/発行者に帰属し、その権利は著作権法によって保護されています。引用にあたっては、著作権法を遵守してご利用ください。

The copyrights of content available on the Keio Associated Repository of Academic resources (KOARA) belong to the respective authors, academic societies, or publishers/issuers, and these rights are protected by the Japanese Copyright Act. When quoting the content, please follow the Japanese copyright act.

Studies on the Thermal Problems of Memory Cores at Their High-Speed Performances

(Received October 23, 1967)

Misao KITAGAWA*

Teruo YOKOYAMA**

Norio EBIHARA***

Abstract

This paper describes a measuring method of the surface temperature of small bodies somewhat above the room temperature and the temperature dependence of switching characteristics of memory cores. The temperature rise of memory cores at high-speed performances has been observed by the method using phosphors, and the relations between the surface temperature rise and the effective temperature rise of cores are obtained. Besides, thermally available criterions are also proposed to estimate the factors affecting the limitations of the cycle time of storage.

I. Introduction

According to the ceaseless requirements for improving the calculating speed of digital computers, the cycle time of storage unit should be as short as possible in accordance with higher efficient performance of circuit components. As a memory element of the main store, the ferrite cores are available at present in large scale computer systems. Several methods to improve the cycle time of memory cores have been proposed as follows; (1) utilization of small size cores, (2) adoption of two-core-per-bit systems,¹⁾ (3) write-in by partial switching and read-out by complete switching.²⁾

As the cycle time is made shorter, the electromagnetic characteristics of memory cores would be comparatively changed owing to heat generation due to hysteresis losses, and thereby the informations stored in them would be altered, or destroyed. Thus the thermal problems about a single core only for the worst case of performances should be investigated at first instead of the thermal problems of a core memory unit.

*北川 節 Associate Professor, Faculty of Engineering, Keio University.

**横山 光男 Instructor, Faculty of Engineering, Keio University.

***海老原 規郎 Graduate Student, Faculty of Engineering, Keio University.

Here is a newly developed method to measure the surface temperature rise by application of phosphors which are much sensitive to temperature change near the room temperature. By this method, the temperature rise of cores and the effects thereof on the switching mechanisms can be easily investigated when the memory cores behave under their higher repetition rate switching.

II. Techniques and devices for core switching

II. 1. Current patterns to drive cores

To investigate the changes in the characteristics of memory cores owing to their internal heating, thermally severe testings should be applied to realize the worst case of performances. Drive current patterns shown in Figures II. 1 (a), (b) and (c) were used for testing. Figure (a) provides a way to observe the flux changes due to the write word current I_{W0} , comparing to the outputs obtained by the patterns in Figure (b) which reveal the complete switching of cores. Figure (c) gives a way to investigate the effects of the bit (information) current I_B on the state "0" which is written by I_{W0} prior to I_B in the core. For the present study, word-organized read and write schemes were adopted. To write "1", therefore, the currents I_{W0} and I_B should be simultaneously provided in the same direction, and to write "0", only the word current I_{W0} is delivered. In varying pulse amplitude and width, t_W , of write current and further repetition rate of read and write cycles, the readout voltages as well as the temperature rises of cores were observed. Read currents through the experiments were selected as their amplitude and pulse width which are large enough to switch the core completely.

II. 2. Drive current generators

To investigate the magnetic and thermal characteristics of cores, drive current generators were made as following specifications :

- (1) Pulse widths vary from 5 to 60 microsec.,
- (2) Repetition rates of the drive currents vary 60 to 150 microsec.,
- (3) Amplitudes of the drive currents vary 100 to 500 mA and 400 to 1000 mA, and
- (4) Rise and fall times have the values within 40 nanosec..

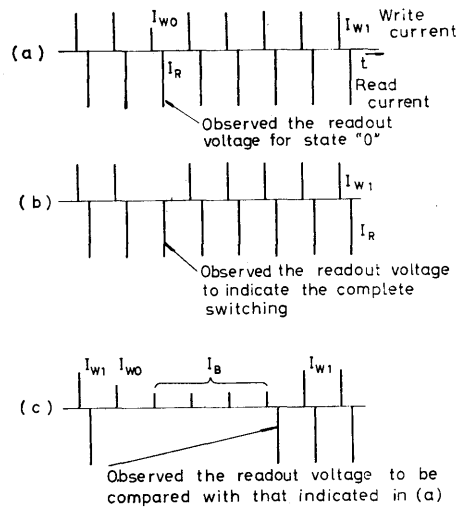


Figure II. 1 Drive current patterns.

III. Measuring devices for surface temperature of cores

There has not been any satisfactory method to measure the surface temperature rise of memory cores until now because of their small dimensions of size.³⁾ The method presented here is to apply the phosphors to memory cores whose luminescent characteristics depend largely upon the temperature change of the cores, and to detect and amplify the intensity changes of the visible lights radiating from the phosphor on the core, which are excited by a particular ultraviolet ray. The surface temperature is obtained graphically by means of the calibration charts which are experimentally prepared.

III. 1. Preparations of phosphors used to measure surface temperature⁴⁾⁵⁾⁶⁾

The luminescent phenomena of phosphors are extremely sensitive to their crystalline structures that most phosphors even with the same constituents might sometimes offer various and different characteristics according to raw materials used and moreover manufacturing techniques adopted.

There may be many combinations between phosphors and impurities added to them. In the experiment calcium oxide was selected as a base of phosphors and bismuth as an impurity.

To make a sample of phosphor to measure the surface temperature, calcium oxide crystals of high purity were prepared as a base of phosphor. Thus calcium nitrate of high purity are put into a platinum melting pot and heated up to 500~600 °C in an electric furnace under the atmospheric pressures. The preheated calcium nitrate are slowly (with the rate of 300°C/hour) heated up again to 800~900°C with the same environment, then kept at the constant temperature about 30 minutes, and cooled down to the room temperature with the same rate of heating.

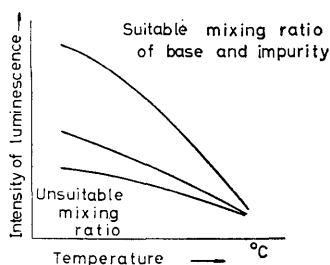


Figure III. 1

Schematic relations between temperature and intensity of luminescence.

As an impurity, bismuth nitrate of 0.01 percent in weight was added to the calcium oxide just prepared above. Thereafter the mixture is slowly heated up to 700~800°C, kept in constant at the state for 30 minutes, cooled down slowly to 80°C, and taken out of the furnace to the atmosphere. The heat cycles repeated thus several times provide a better sample of phosphor which emits more intense luminescence. This phosphor shows a white luminescence when excited by an ultraviolet ray of 3650 Angstrom. Figure III. 1 shows typical characteristics of the temperature dependence upon the intensity of luminescence.

III. 2. Measuring techniques of surface temperature by means of the phosphor

The processes to measure the temperature rise of the core under test are as follows :

- (1) The phosphor prepared above is painted partially on the core surface,
- (2) The core under test is heated with the hysteresis losses caused by the switching currents,
- (3) Under the above condition, the phosphor painted on the sample core is illuminated with the ultraviolet ray of wave length 3650 Angstrom, and
- (4) The visible lights emitted from the excited phosphor are received and amplified by the photomultiplier tube, and its anode current variations are measured by a micro-micro-ammeter.

The measuring devices for the surface temperature of core is shown schematically in Figure III. 2. The ultraviolet ray of 3650 Angstrom, which is emitted from an ultraviolet lamp through the filter 1 composed of an UVD-1 and an UV-35, illuminates and excites the phosphors painted on the core under test. The visible lights emitted from the excited phosphors are introduced to a glass tube which is silver-gilt on its outer surfaces, passed through the filter 2 of UY-48, and received at the photomultiplier tube mounted in the dark box 2. In the figure, the dark boxes 1 and 2 are provided to avoid the external undesirable lights.

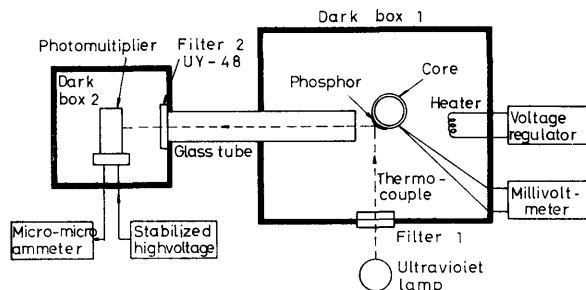


Figure III. 2 Temperature measuring devices of memory core by means of phosphor.

The glass tube has much advantages so easy to introduce the visible lights from the phosphors on a small body like a memory core to the photomultiplier, even under considerable deviations from the relative positions between them. Figure III. 3 shows an example of the calibration charts, which is made to

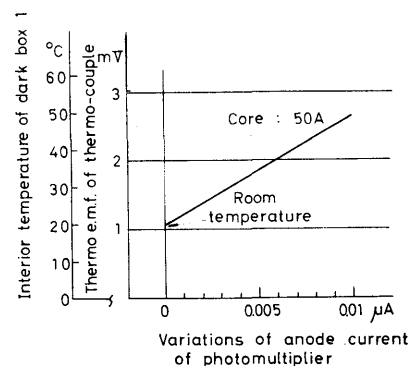


Figure III. 3 Calibration chart.

show the change of anode currents against the interior temperature of the dark box 1, measured by the thermo-couples.

IV. Experimental results and considerations

Memory cores tabulated below are selected as test samples to investigate the temperature rise of cores due to their hysteresis losses.

*Materials	Nominal size	80-mil	50-mil	30-mil
		80A	50A	30A
A			50B	
B				30C
C				

*All cores are Mn-Mg ferrites but different in minute constituents labeled as A, B, and C.

The results obtained are shown in Figures IV. 1 to IV. 7, where the critical bit current I_B and the word current I_{W0} are defined as follows:

Critical bit current I_{BM} : Maximum bit current I_B not to disturb the magnetized state of "0".

Critical word current I_{W0M} : Maximum word current I_{W0} , which generates the 1/3 peak voltage of the output which is read from the magnetized state of "1".

IV. 1. Switching phenomena of cores

Figure IV. 1 shows the hysteresis characteristics of the core 50A, which is obtained experimentally under the condition neglected the hysteresis losses, and calculated from the output waveforms and the drive currents. Figure IV. 1 also indicates that

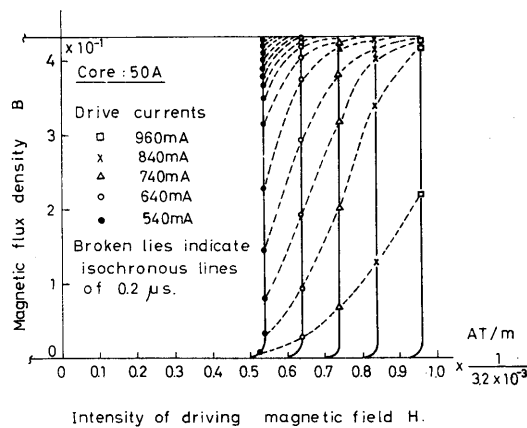


Figure IV. 1 Hysteresis curves due to pulse drive currents.

the switching behaviors of fluxes by pulse currents undergo slowly because of the time delay due to the domain wall rotations, even though the magnetizing currents reach their saturated magnitudes, and that the rates of flux changes becomes faster as the drive currents get larger in magnitude. Broken lines in the figure which show the isochronous lines of each 0.2 microseconds suggest that the switching time for the saturated flux density can be considerably shortened.

Figures IV. 2 (a) and (b), which show the behaviors of isochronous lines on the hysteresis curves due to the variations of environment temperature of cores, indicate that the more temperature is raised, the faster becomes switching speed of flux and the more becomes considerable flux change at the leading edge of the drive pulse current.

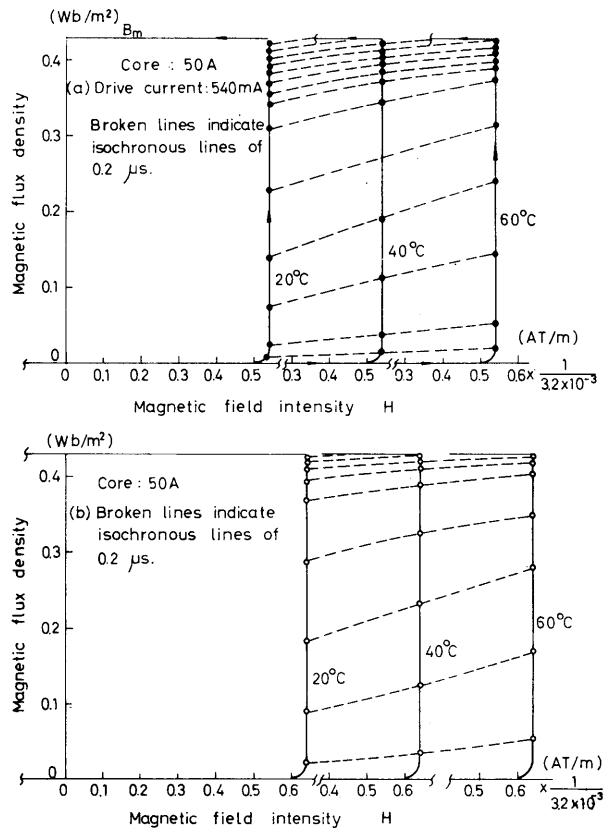


Figure IV. 2 Variations of hysteresis curves due to the environment temperatures.

Figures IV. 3 (a) and (b) show that the peak output voltages due to the switching magnetizations are generally proportional to the switched fluxes to some extent, but that above a certain total flux change the switching speed gets rather slower

and thus the output voltage becomes correspondently smaller. These phenomena indicate the existence of the so-called over-saturated magnetizations resulted from the intense magnetizing fields.⁷⁾⁸⁾⁹⁾

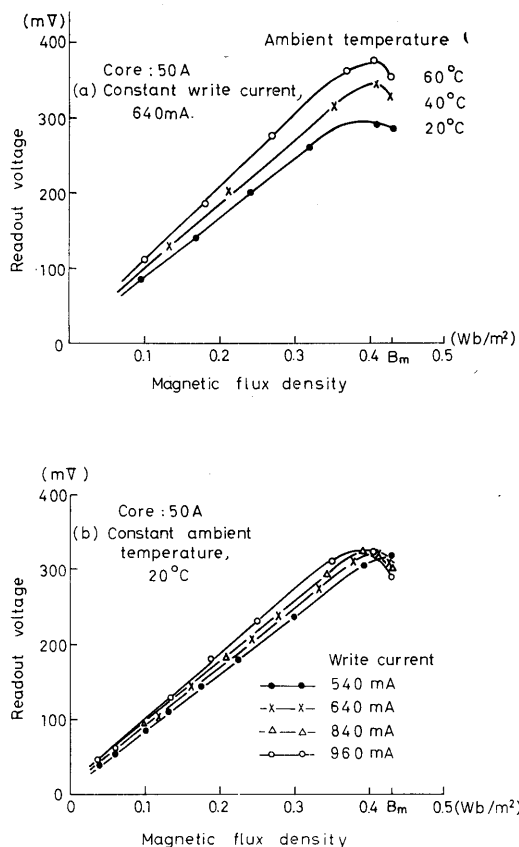


Figure IV. 3 Readout voltage vs. amounts of switched fluxes of magnetization by varying ambient temperature and write current amplitude respectively.

Figure IV. 4 shows that the effects of bit current I_B in the amounts of switched fluxes, that is, those of magnetizations by the bit current pulses, which are supplied 11 times of 12 in the some direction without flowing the word current I_{W0} , and are studied by varying the pulse width of bit current I_B for the specified current amplitudes.

Figure IV. 5 indicates the effects of magnetization by additive bit current I_B on the magnetization by a single word current I_{W0} provided prior to the application of I_B . In the figure, the magnetization by I_{W0} is normalized as the flux density B (Wb/m²), and the critical value of the bit current I_B also as the field intensity H (AT/m) to to compare the effects of the superposed magnetizations by the bit currents.

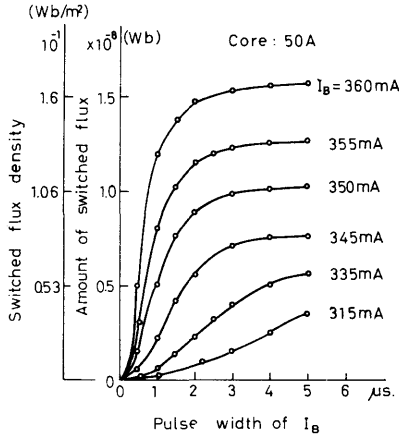


Figure IV. 4 Bit current vs. amounts of switched flux.

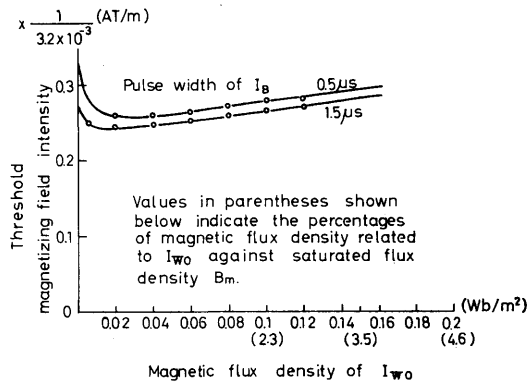


Figure IV. 5 Threshold magnetizing current (field) vs. magnetic flux density corresponding to I_{w0} .

IV. 2. Temperature rises of memory cores due to internal heating

The internal heating of memory cores is due to the hysteresis losses which are generated during the memory cycles. The energy loss per unit volume, w_h , dissipated within the core can be expressed in the equation

$$w_h = \oint H dB \quad (\text{W/m}^3), \quad (1)$$

where H (AT/m) is the applied magnetic field intensity and B (Wb/m²) the magnetic flux density within the core respectively. When the core is switched completely

by alternating current pulses, the energy loss per unit volume is expressed approximately

$$w = 2HB_m f, \quad (\text{W/m}^3) \quad (2)$$

where B_m (Wb/m²) is the saturated flux density, and f (Hz) the repetition rate of alternating current pulses.

If the internal temperature gradient within the core be neglected, the temperature rise of core θ (deg.) is considered to be proportional to its internal energy losses, and so

$$\theta = \frac{W_i}{kS} = \frac{wV}{kS}, \quad (3)$$

where W_i (W) is the total energy loss of the core, S (m²) the cross-sectional area perpendicular to the circular magnetic paths of the core, V (m³) the volume of the core, and k the proportional constant.

Each of the 30-, 50-, and 80-mil cores is assumed to have the identical magnetic properties. In the case when each core be driven with the same repetition rate and the same magnetic field intensity within the range of complete switching behavior, the energy loss of each core per unit volume and per unit time can be considered identical. But the temperature rise of each core, however, could not be identified because of the different ratios of both surface areas and volumes. Drive current ratios which give the same energy loss per unit volume can be calculated from the data on B_m 's and the ratios of the mean magnetic paths of three kinds of core sizes as shown in Table IV. 1. Therefore, the drive current for each core necessary to give the same energy loss per unit volume should have the ratios tabulated in Table IV. 1 and selected to have the amplitude and pulse width to behave as a complete switching. An example for repetition rate of 500kHz is shown in Table IV. 2.

Table IV. 1 Temperature rise ratios and drive current ratios.

Core	30 A	50 A	80 A
Surface area ratios	1	4	12
Volume ratios	1	6	33
Temperature rise ratios	1	1.5	2.75
B_m (Wb/m ²)	0.25	0.43	0.47
Mean magnetic path ratios	1	1.6	2.6
Drive magnetic field intensity ratios	1	0.59	0.53
Drive current ratios	1	0.94	1.37

Table IV. 2 Temperature rise of magnetic core (not calibrated).

Core	30 A	50 A	80 A
Heat generated within the core per unit volume, w (W/m ³)	5.5×10^6	5.5×10^6	5.5×10^6
Heat generated within the core, W_i (W)	$3.6 \cdot 10^{-3}$	$17 \cdot 10^{-3}$	$120 \cdot 10^{-3}$
Temperature rise (deg.), measured	2	5	14

The temperature rise shown in Table IV. 2 is measured by the method using phosphors mentioned above. The experimental values of the temperature rise seem to give much higher ratios than those expected from Table IV. 1. Thus it means that the temperature rises are much more remarkable with larger dimensions of cores.

Experimental results of the temperature rises measured at some 50-mil cores are shown in Figures IV. 6 (a), (b), and (c), where the readout voltage of state "1", the critical values of the bit current I_B and word current I_{W0} are also shown as function of the repetition rates of the drive currents for each case of various pulse widths of write currents.

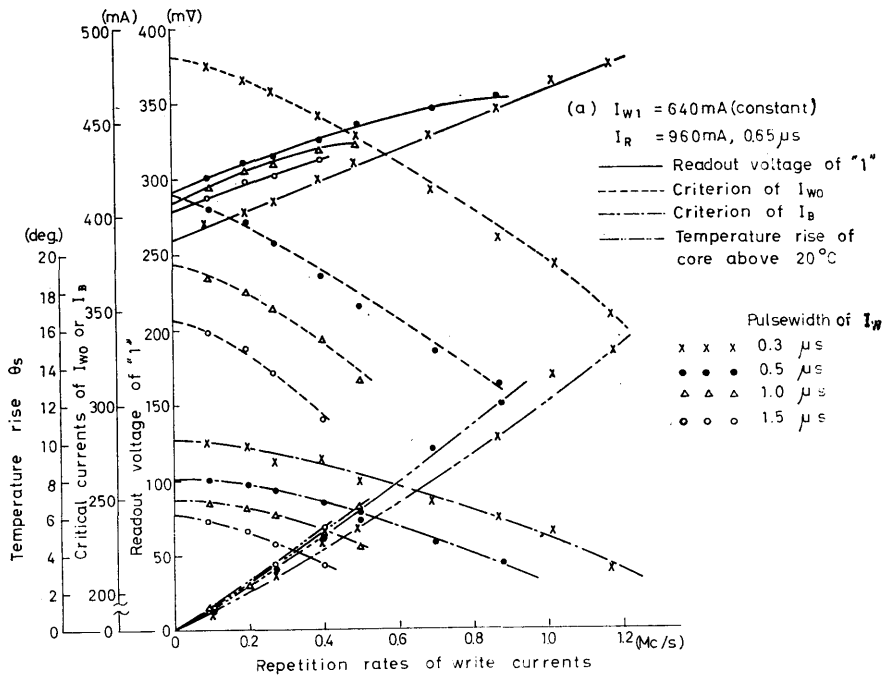


Figure IV. 6 (a) Thermal and switching characteristics of ferrite core.

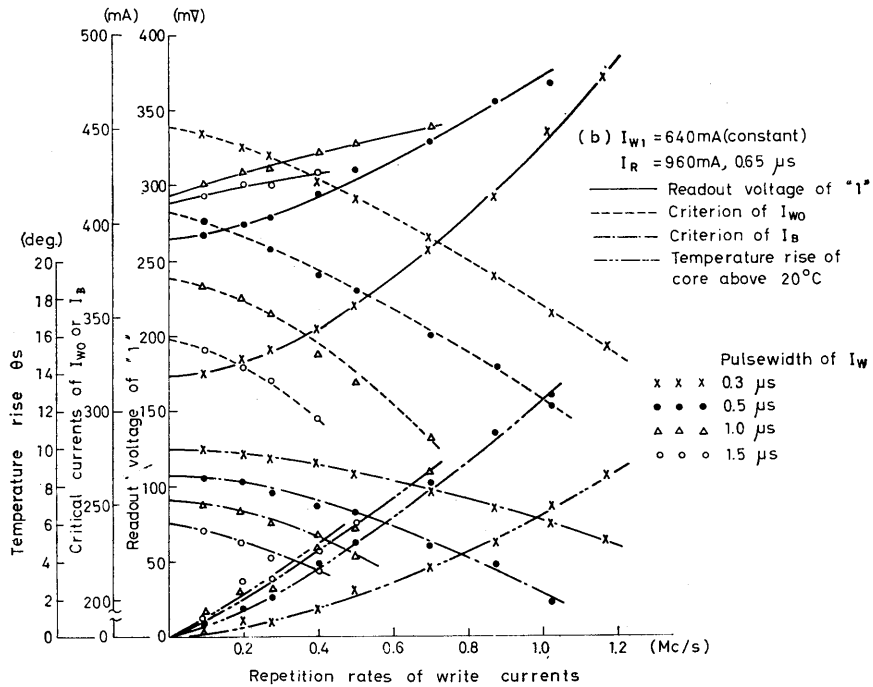


Figure IV. 6 (b) Thermal and switching characteristics of ferrite core.

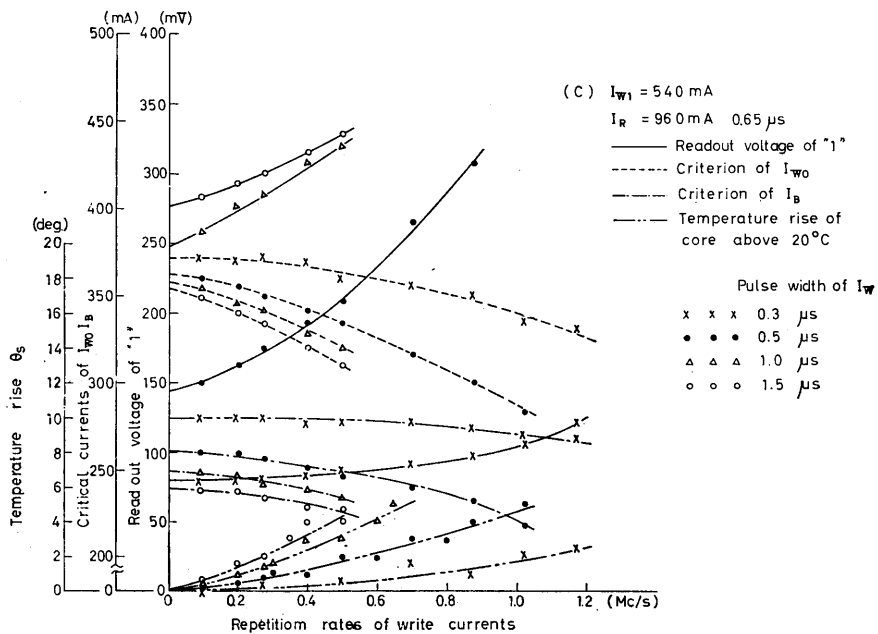


Figure IV. 6 (c) Thermal and switching characteristics of ferrite core.

IV. 3. Effective temperature and surface temperature of core

The temperature measured by the method using phosphors corresponds to the surface temperature of core, and does not indicate its average effective temperature. To obtain the relationship between the effective and the surface temperatures, the same output voltages of state "1" of the core during the switching magnetizations are adopted as a measure to connect the temperature rise due to the hysteresis losses to the ambient temperature of the core in the case of negligible hysteresis losses.

Figure IV. 7 shows that the relationship between the surface temperature rise θ_s and the effective temperature rise θ_e is expressed by

$$\theta_e = 3.5 \theta_s. \quad (4)$$

This fact tells the core has a considerable temperature gradient between the surface and the middle part of its body, even though it has a particularly small sizes.

IV. 4. Thermally available criterions of memory cores

Figures IV. 8 (a) and (b) shows the thermally available criterions of 50-mil and 30-mil cores respectively, with regards to the write current I_w (that is $I_{w0} + I_R$) and read current I_R by varying their pulse widths and repetition rates. The available criterion characteristics, for instance, as shown in Figure IV. 8(a) for 50-mil core can be obtained graphically from Figures IV. 6(a), (b), and (c).

There exist several causes to limit the reductions of the repetition period (or cycle time). These are : (1) the direct effect decided from the pulse widths of I_w and I_R , (2) the reduction of the readout voltages caused by decreasing the amount of the switching magnetic fluxes of core resulted from narrowing the pulse width of I_w , (3) the reduction of maximum values of I_{w0} and I_R defined previously as critical values because of the temperature rise of cores, and so forth.

To reduce the repetition period, it should be noted that the write "1" current I_{w1} has a large amplitude and a narrow pulse width to be able to perform the partial switchings, but too larger amplitude of I_{w1} makes the available criterions narrower and gives an undesirable effects to the stability of memory cycles. Thus any shorter repetition period suited for each core can be experimentally deduced. About 540mA would be suited for 30- and 50-mil cores respectively and 640 mA for 80-mil core.

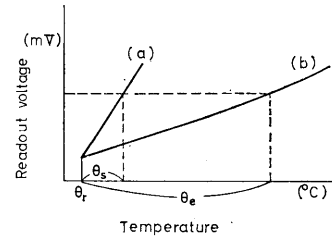


Figure IV. 7

Procedure to obtain the effective temperature rise of core. Curve (a) represents the output voltages of "1" vs. surface temperature rise of core due to internal heating.

Curve (b) represents the output voltages of "1" vs. ambient temperature in case of negligible internal heat losses.

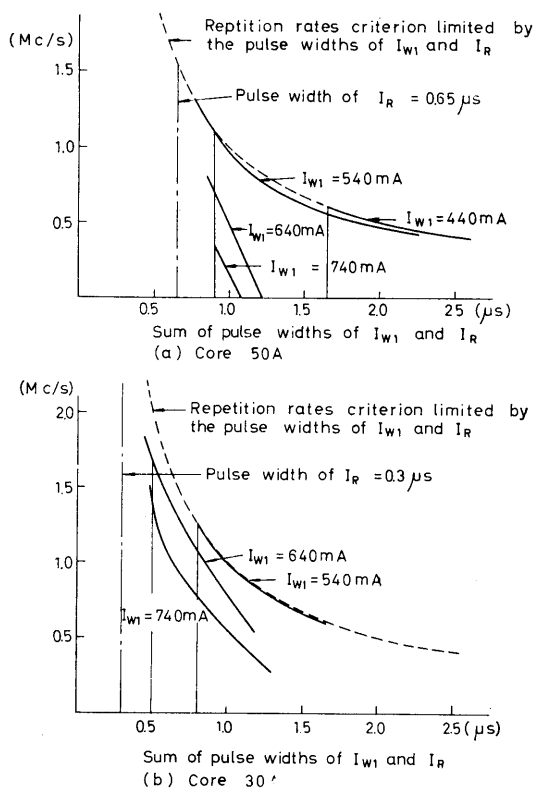


Figure IV. 8 Thermally available criterions of cores.

IV. 5. Calculations of the temperature rises within the core

The Fourier differential equation related to the heat transfer may be applied to calculate the internal temperature distributions of core. It is reasonably assumed that the core be a hollow cylinder and within the body the heat sources may be uniformly distributed, then

$$\partial\theta/\partial t = \nabla^2\theta \lambda / c\rho + Wc\rho, \quad (5)$$

where θ (deg.) is the temperature of the hollow cylinder, λ (W/m·deg.) the heat conductivity, c (kW/4.2·s·kg·deg.) the specific heat, ρ (kg/m³) the density, and W (W/m³) the heat generated within the cylinder per unit volume per unit time.

It is assumed that the temperature obtained by our method is the surface temperature of core which is constant all over the surface. If, here, the temperature within the core be expressed by the temperature between the surface and the point considered, the boundary conditions become fairly simpler. If only the temperature distributions of the stationary state be considered, the left-hand term of equation (5) will be reduced to zero, hence

$$(18)$$

$$\nabla^2 = -W/\lambda. \quad (6)$$

Expressing by the cylindrical coordinates, equation (6) is written as

$$\frac{1}{r} \frac{\partial}{\partial r} \left(r \frac{\partial \theta}{\partial r} \right) + \frac{1}{r^2} \frac{\partial^2 \theta}{\partial \varphi^2} + \frac{\partial^2 \theta}{\partial z^2} = -\frac{W}{\lambda}. \quad (7)$$

Variables in equation (7) are shown in Figure IV. 9, and temperature distributions are independent of ρ , so equation (7) becomes

$$\frac{\partial^2 \theta}{\partial r^2} + \frac{1}{r} \frac{\partial \theta}{\partial r} + \frac{\partial^2 \theta}{\partial z^2} = -\frac{W}{\lambda} \quad (8)$$

under the following condition

$$\theta = 0 \text{ at } r = r_1, r = r_2, \text{ and } z = \pm z_0. \quad (9)$$

Solving equation (8) for θ gives

$$\theta = \sum_{n=0}^{\infty} \{ c_n \cdot \cos(a_n z) \cdot [I_0(a_n r) + \eta_n K_0(a_n r)] \} - (W/2\lambda)(z^2 - z_0^2), \quad (10)$$

where $I_0(x)$ is the zero order 1st class modified Bessel functions and $K_0(x)$ the zero order 2nd class modified Bessel functions, and a_n , c_n , and η_n should be determined to satisfy the boundary condition (9).

Generally, the temperature distributions of the hollow cylinder are given in the following form

$$\begin{aligned} \theta = \frac{W}{\lambda} \left\{ \sum_{n=1}^{\infty} \left[-\frac{2}{a_n^3 z_0} \cdot \sin(a_n z_0) \cdot \frac{1}{I_0(a_n r_1) + \eta_n K_0(a_n r_1)} \cdot \cos(a_n z) \right. \right. \\ \left. \left. \times (I_0(a_n r) + \eta_n K_0(a_n r)) \right] - \frac{1}{2} (z^2 - z_0^2) \right\}, \end{aligned} \quad (11)$$

$$\text{where } a_n = \pi/2z_0(2n-1) \quad (12)$$

$$\eta_n = -\frac{I_0(a_n r_1) - I_0(a_n r_2)}{K_0(a_n r_1) - K_0(a_n r_2)}, \quad n = 1, 2, 3, \dots \quad (13)$$

First of all, the heat conductivity λ of the core should be calculated under the assumptions that the temperature measured by the method is the surface temperature of core and that the effective temperature deduced from the temperature characteristics of core means its average value. Equation (11) may be written for simplicity as

$$\theta = \frac{W}{\lambda} \Theta(r, z). \quad (14)$$

The average temperature of core, $\theta_{av}(\text{deg.})$, can be expressed as

$$\theta_{av} = \frac{1}{2z_0(r_2 - r_1)} \int_{r_1}^{r_2} \int_{-z_0}^{z_0} \theta dr dz. \quad (15)$$

From equations (14) and (15), the heat conductivity can be expressed in the form

$$(19)$$

$$\lambda = \frac{1}{\theta_{av}} \cdot \frac{W}{2z_0(r_2 - r_1)} \int_{r_1}^{r_2} \int_{-z_0}^{z_0} \theta dr dz. \quad (16)$$

As an example, 80-mil core is put to calculate the heat conductivity of the core for

$$\begin{aligned} r_1 &= 0.655 \cdot 10^{-3} \text{ (m)}, \\ r_2 &= 1.025 \cdot 10^{-3} \text{ (m)}, \text{ and} \\ z_0 &= 0.325 \cdot 10^{-3} \text{ (m)}. \end{aligned}$$

$\theta(r, z)$ corresponding to the terms in equation (11) were computed by the digital computer K-1 (home-made in 1958) for those points regarding

$$\begin{aligned} r &= r_1 + (r_2 - r_1)p/6 & p &= 0, 1, 2, 3, 4, 5, 6 \\ z &= (z_0 q)/6 & q &= 0, 1, 2, 3, 4, 5, 6 \end{aligned}$$

and thus the right-hand term of Equation (15) calculated by the Simpson's method results in

$$\theta_{av} = (W/\lambda) \cdot (0.0074) \cdot 10^{-3} \text{ (deg.)}.$$

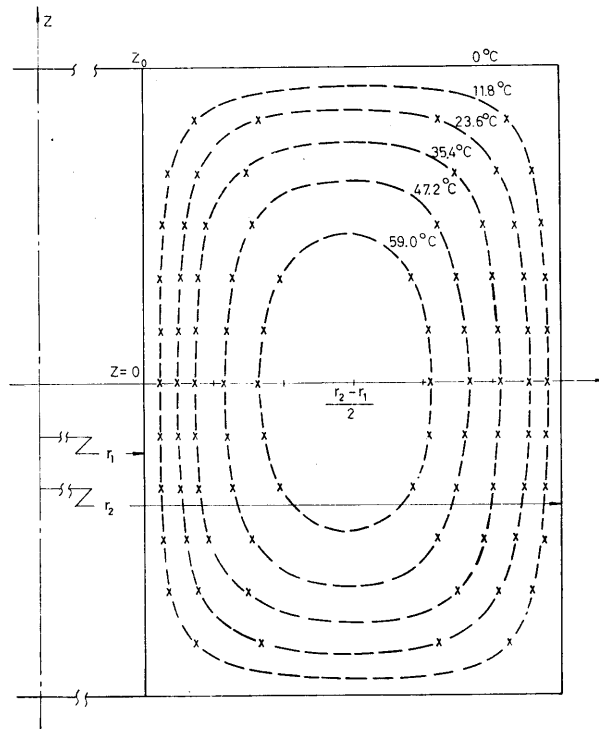


Figure IV. 9 Temperature distributions within the core which were calculated from Equation (11). Values shown in the figure are temperature rise above surface one.

On the other hand, from equation (4) and Table IV. 2

$$\theta_{av} = 14 \cdot (3.5 - 1) \text{ (deg.)}$$

$$W = 5.5 \cdot 10^{-6} \text{ (W)}$$

are substituted for the terms in equation (16), and then

$$\lambda = 1.16 \text{ (kW/4.2} \cdot \text{s} \cdot \text{kg} \cdot \text{deg.)}.$$

Applying the heat conductivity to equation (11), the temperature distributions of the cross-sectional areas of core were calculated except near the innermost part of it. The computed results are drawn in Figure IV. 9 with the broken lines, which indicate a considerable temperature gradient between the surface and the inner part of the core.

V. Conclusion

A measuring technique of the surface temperature for a small body like magnetic memory core is developed by using the phosphor to estimate the effects of heating due to the hysteresis losses of core and the relationship between the surface and the effective temperatures of core has been experimentally obtained introducing the identical readout voltage as a measure of calibration.

Thereafter, thermally available criterions for memory cores of several sizes are investigated and it is recognized that the memory cycle time can be reduced considerably by utilizing the partial switchings with smaller pulse widths and larger pulse amplitudes.

On the other hand, the internal temperature distributions of core are calculated to estimate the internal temperature gradient in a core, and thus it is concluded experimentally that the effective, or average temperature of core may become 3.5 times more than that of the surface.

Additionally the temperature measuring technique thus developed has some advantages to measure the surface temperature on a small portion of a small body such as integrated circuits slightly above the room temperature. The glass tube to introduce lights may be replaced by optical fibers.

VI. Acknowledgement

This study has been accomplished by the aid from the Keio-Gijuku Fukuzawa Memorial Foundations for Science and Research Developments, for which authors express their deep acknowledgements. Authors express their sincere gratitudes to Professor Tomoyuki Somiya and Professor Shigeo Sasaki for directing and encouraging their studies, and also are thankful to Professor Toshio Horiuchi and Associate Professor Shoichi Kurita for their fruitful advices to prepare and develop the phosphors of high purity and sensitivity.

Reference

1. W. H. Phodes, L. A. Russell, F. E. Sakalay, and R. M. Whalen. "0.7 Microsecond Ferrite Core Memory", IBM Journal, 174 (July, 1961).
2. R. H. Trancrell and R. E. McMahon, "Studies on Partial Switching of Ferrite Cores", J. Appl. Phys., 31, 762 (1960).
3. K. Tsuchiya and K. Yamada, "On the Thermal Problems of Memory Cores Accompanied by High-Speed Performances", I. E. E. of Japan Conventions, 712 (April, 1965).
4. Lee C. Bradley, "A Temperature-Sensitive Phosphor Used to Measure Surface Temperature", RSI, 24, 3 (March, 1953).
5. J. Ewles and Lee, "Studies on the Concept Large Activated Centers in Crystal Phosphors", J. Electrochemical Society, 100, 9 (September, 1953).
6. H. C. Froelich, "Copper-Activated Zinc Sulfide Phosphors with Trivalent Substituents", J. Electrochemical Society, 100, 11 (November, 1953).
7. F. Chikazumi, "Physical Properties of Ferromagnetic Materials", (book).
8. H. Saito and Y. Shichijo, "Ferrites", (book).
9. N. Menyuk and J. B. Goodenough, "Magnetic Materials for Digital Computer Components", J. Appl. Phys., 26, 1 (January, 1953).